Cell

α2A-Adrenoceptors Strengthen Working Memory Networks by Inhibiting cAMP-HCN Channel Signaling in Prefrontal Cortex

Min Wang,[1] Brian P. Ramos,[1] Constantinos D. Paspalas,[1,4] Yousheng Shu,[1] Arthur Simen,[2] Alvaro Duque,[1] Susheel Vijayraghavan,[1] Avis Brennan,[1] Anne Dudley,[1] Eric Nou,[1] James A. Mazer,[1] David A. McCormick,[1,3] and Amy F.T. Arnsten[1,3,*]
[1] Department of Neurobiology
[2] Department of Psychiatry
[3] The Kavli Institute of Neuroscience
Yale University School of Medicine, New Haven, CT 06510 USA
[4] Division of Neuroanatomy, University of Crete School of Medicine, Heraklion, Greece
*Correspondence: amy.arnsten@yale.edu
DOI 10.1016/j.cell.2007.03.015

SUMMARY

Spatial working memory (WM; i.e., "scratch-pad" memory) is constantly updated to guide behavior based on representational knowledge of spatial position. It is maintained by spatially tuned, recurrent excitation within networks of prefrontal cortical (PFC) neurons, evident during delay periods in WM tasks. Stimulation of postsynaptic α2A adrenoceptors (α2A-ARs) is critical for WM. We report that α2A-AR stimulation strengthens WM through inhibition of cAMP, closing Hyperpolarization-activated Cyclic Nucleotide-gated (HCN) channels and strengthening the functional connectivity of PFC networks. Ultrastructurally, HCN channels and α2A-ARs were colocalized in dendritic spines in PFC. In electrophysiological studies, either α2A-AR stimulation, cAMP inhibition or HCN channel blockade enhanced spatially tuned delay-related firing of PFC neurons. Conversely, delay-related network firing collapsed under conditions of excessive cAMP. In behavioral studies, either blockade or knockdown of HCN1 channels in PFC improved WM performance. These data reveal a powerful mechanism for rapidly altering the strength of WM networks in PFC.

INTRODUCTION

There are multiple forms of memory mediated by distinct brain systems: e.g., long-term consolidation of declarative memories mediated by hippocampal circuits, repetitious experience creating habit memories in striatal loops, and varying types of associative memories stored in the cortex, amygdale, and cerebellum. In contrast to these enduring forms of memory, working memory (WM) maintains information in a temporary buffer that is constantly updated according to cognitive demands. WM depends on the prefrontal cortex (PFC), a highly evolved brain region that is greatly expanded in human and nonhuman primates. The contents of WM can be recalled from long-term storage or can represent a recent event that is temporarily held in mind. This represented information is used to guide behavior, thought, and emotion, allowing us to inhibit inappropriate actions and to plan for the future (Fuster, 1985; Goldman-Rakic, 1995). Given the short-term nature of WM, it is unlikely to involve the types of synaptic structural changes thought to underlie consolidation of long-term memory. Rather, WM is thought to arise from recurrent activity in a network of PFC neurons with shared properties (Goldman-Rakic, 1995).

The spatial WM characteristics of neurons in the primate PFC (area 46) have been well characterized in monkeys performing spatial WM tasks that require the animal to remember a constantly changing, visually cued spatial location over a brief delay period. Goldman-Rakic (1995) identified a canonical PFC microcircuit with spatially tuned mnemonic delay period activity. The key features of the PFC microcircuit are (1) persistent activity created by mutual excitation between pyramidal neurons with similar spatial properties, and (2) spatial tuning regulated by inhibitory interneurons with dissimilar spatial properties. The horizontal connectivity of layer III pyramidal cells is thought to be an important component of the PFC microcircuit (Kritzer and Goldman-Rakic, 1995). Recurrent connections allow PFC neurons to continue firing during the delay period when no stimulus is present in the environment, maintaining representations over time even in the presence of distracting stimuli (Miller et al., 1996). This is a fragile process that is highly dependent on the correct neurochemical environment.

Catecholamines have an essential influence on PFC spatial WM functions. Although early work focused on dopamine, it is now known that norepinephrine (NE) strongly influences WM via postsynaptic α2A-adrenoceptors (α2A-ARs) (Arnsten and Goldman-Rakic, 1985; Franowicz et al., 2002). Blockade of these receptors in PFC profoundly impairs spatial WM (Li and Mei, 1994) and erodes delay-related firing of PFC neurons (Li et al., 1999). Conversely, stimulation of postsynaptic α2A-ARs strengthens PFC cognitive functions in rodents (Franowicz et al., 2002), monkeys (Arnsten et al., 1988), and humans (Jakala et al., 1999). Based on this research, the α2A-AR agonist, guanfacine, is currently used to treat PFC cognitive deficits in patients with Attention Deficit Hyperactivity Disorder (ADHD) (Scahill et al., 2001; Taylor and Russo, 2001), Tourette's Syndrome (Scahill et al., 2001), and mild traumatic brain injury (McAllister et al., 2004). However, the cellular basis and molecular events underlying these therapeutic actions are not known.

Recent studies indicate that elevated cAMP signaling in PFC impairs behavioral measures of WM, and that α2A-AR stimulation improves WM performance via Gi suppression of cAMP intracellular signaling. In contrast to long-term memory consolidation which is facilitated by cAMP signaling, WM performance at short delays is impaired by increased cAMP signaling, e.g., following infusion of the cAMP analog, Sp-cAMPS, into the rat PFC (Taylor et al., 1999). Similarly, WM performance of aged monkeys is impaired by systemic administration of the phosphodiesterase 4 (PDE4) inhibitor, rolipram, which increases endogenous levels of cAMP (Ramos et al., 2003). The enhancing effects of guanfacine on WM can be blocked by coinfusion of low dose Sp-cAMPS in the rat PFC (Ramos et al., 2006). Conversely, inhibition of cAMP with Rp-cAMPS infusions improved WM performance (Ramos et al., 2003). These findings indicate that excessive cAMP actions in PFC impair WM. Importantly, dysregulated cAMP signaling may contribute to WM deficits in schizophrenia, as a gene linked to this disorder, DISC1, has been found to upregulate PDE4B activity under conditions of high cAMP production (Millar et al., 2005). Thus it is key to understand how elevated cAMP signaling impairs PFC cognitive operations.

Although cAMP is often associated with protein kinase A, it also has powerful influences on Hyperpolarization-activated Cyclic Nucleotide-gated (HCN) channels that pass an h current (Ih) when opened. In neocortex and hippocampus, Ih channels are heteromers of HCN1 and HCN2 subunits that are highly responsive to cAMP (Chen et al., 2001; Ulens and Tytgat, 2001). They are localized on distal pyramidal dendrites (Lörincz et al., 2002; Notomi and Shigemoto, 2004), and have important effects on neuronal excitability (Day et al., 2005; Fan et al., 2005; Poolos et al., 2002) and dendritic integration in hippocampus (Magee, 1999). As pyramidal cells have a negative resting potential (~ -65 mv), HCN channels are thought to open during the awake, resting state in the presence of cAMP (Nolan et al., 2004). In hippocampus, inputs to CA1 pyramids are spatially segregated such that the opening of Ih channels on distal dendrites functionally disconnects CA1 pyramidal cells from CA3 inputs without influencing perforant path connections (Nolan et al., 2004). Ih channels may have similarly powerful effects on PFC function, given the importance of dendritic inputs for sustaining recurrent excitation during the delay period of WM tasks. Ih channels are particularly dense on pyramidal dendrites of the superficial cortical layers (Lörincz et al., 2002; Notomi and Shigemoto, 2004). In monkey PFC, these layers also contain the highest concentration of α2A-ARs, localized in axons, dendritic spines and shafts (Aoki et al., 1998; Goldman-Rakic et al., 1990).

This study demonstrates that HCN1 or HCN1/HCN2 heteromers on spines of pyramidal dendrites are spatially coexpressed with the α2A-AR, thus providing a potent substratum for functional interaction in the primate PFC. Electrophysiological and cognitive experiments support a model where α2A-AR agonists such as guanfacine improve PFC cognitive function by inhibiting the production of cAMP, closing HCN channels, and strengthening the PFC networks that underlie delay-related cell firing in monkeys performing a spatial WM task.

RESULTS

α2A-AR Stimulation Strengthens Delay-Related Firing of PFC Neurons during WM Tasks

Monkeys performed an oculomotor spatial delayed response (ODR) task, illustrated in Figure 1A. The ODR task requires the monkey to make a memory-guided saccade to a visuo-spatial target. Neurons were recorded from area 46 of the dorsolateral PFC (Figure 1B) as the monkey performed the task. Figure 1C shows the activity of a PFC neuron with task-related firing. This neuron shows delay-related firing for the 180° location (preferred direction) but not for other directions (e.g., 0°, nonpreferred direction). In the present study, 128 neurons with delay-related mnemonic activity were isolated and subjected to iontophoretic application of pharmacological agents (see the Supplemental Data, available with this article online, for tables summarizing the effects of drugs [Table S1] and their reversal [Table S2] on PFC neuronal response).

Intra-PFC administration of the α2A-AR agonist, guanfacine, improves WM performance (Mao et al., 1999). However, guanfacine has never been examined for its effects on PFC neuronal firing. In the present study, guanfacine was applied iontophoretically to 35 neurons with spatial delay-related activity. Low doses of guanfacine (5–15 nA) significantly enhanced delay-related activity for the preferred direction in 28 out of 35 cases, while having no effect on neuronal activity of the remaining 7 neurons. In contrast, high doses of guanfacine (20–50 nA) suppressed delay-related activity in nine out of nine neurons, perhaps due to stimulation of presynaptic α2A-ARs, reducing endogenous NE release.

Figure 2A shows a PFC neuron with relatively weak spatial mnemonic tuning in the control condition. Following

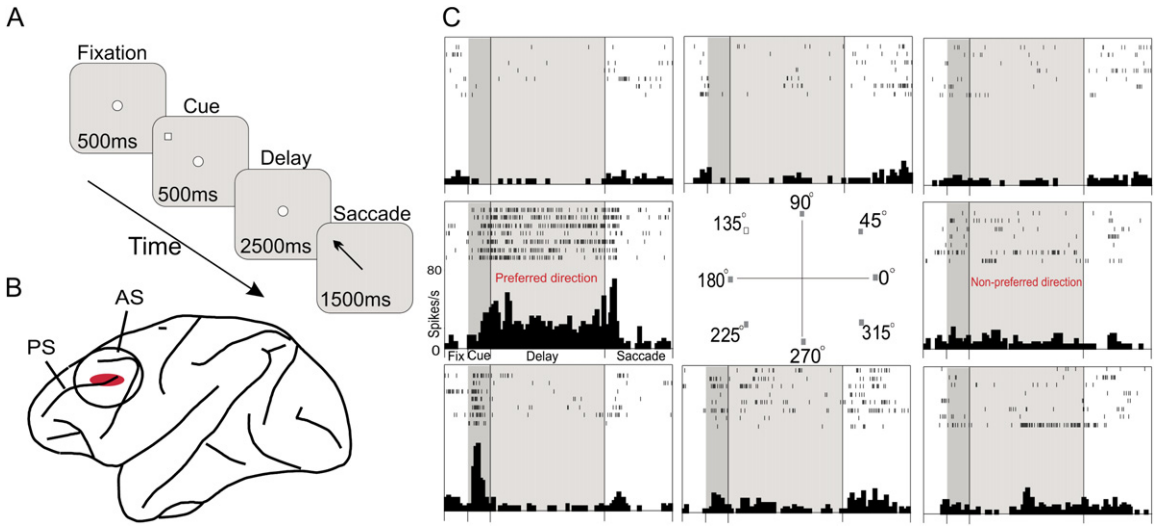

Figure 1. The WM Paradigm Used for Electrophysiological Recordings

(A) ODR task: Trials began when the monkey fixated on a central point for 0.5 s. A cue was present in 1 of 8 possible locations for 0.5 s and was followed by a delay period of 2.5 s. When the fixation point was extinguished, the monkey made a saccade to the location of the remembered cue.

(B) Position of the cylinder (big circle) and the region of electrophysiological recording in dorsolateral PFC (red area). PS: principal sulcus; AS: arcuate sulcus.

(C) Neuronal activity of a PFC cell on the ODR task. Rasters and histograms are arranged to indicate the location of the corresponding cue. This cell exhibited significant delay-related activity for the 180° location (preferred direction) but not for other directions (e.g., 0°, nonpreferred direction).

guanfacine application (10 nA), delay-related firing was substantially increased for the preferred (one-way ANOVA, $p < 0.0001$) but not for the nonpreferred direction ($p > 0.05$), thus enhancing spatial mnemonic tuning. In neurons with strong spatial mnemonic tuning, the effects of guanfacine (5 nA) were similar but smaller in magnitude, as shown in Figure 2B ($p < 0.001$). At higher doses, guanfacine (50 nA) did not have enhancing effects (Figure 2B).

Previous studies demonstrated that iontophoretic application of yohimbine, an α2-AR antagonist, suppressed delay-related firing in PFC neurons (Li et al., 1999). Replicating these previous reports, iontophoresis of yohimbine (15 nA) suppressed delay-related activity for the preferred direction, thus eroding spatial mnemonic tuning ($p < 0.0001$, Figure 2C). The suppressive effects of yohimbine on delay activity occurred in 15 out of 15 cases ($p < 0.01$ for each cell). Furthermore, coiontophoresis of yohimbine (15 nA) reversed the enhancing effects of guanfacine on delay-related activity ($p < 0.01$, Figure 2D), consistent with actions at α2-ARs (population responses for guanfacine and yohimbine alone can be seen in Figures 2E and 2F, respectively). These results indicate that endogenous NE stimulation of α2-ARs plays an important role in strengthening delay-related firing.

cAMP Suppresses PFC Neuronal Firing during Memory Tasks

Behavioral studies in rats have shown that amplification of cAMP actions with Sp-cAMPS impaired spatial WM, while inhibition of cAMP actions with Rp-cAMPS ameliorated WM deficits. Consistent with these behavioral results, we found that iontophoresis of Sp-cAMPS (10 nA) significantly decreased delay-related firing for the preferred direction ($p < 0.001$, Figure 3A). Although the suppressive effects of Sp-cAMPS were replicated in 13 out of 27 neurons, Sp-cAMPS was found to nonspecifically increase the neuronal firing in 9 of 27 neurons, and had no effect in 5 neurons. These effects may result from Sp-cAMPS blocking adenosine receptors, inducing a nonspecific increase in firing rate. Thus, we examined an alterative method for increasing cAMP signaling. Etazolate is a PDE4 inhibitor that increases cAMP levels by inhibiting the breakdown of endogenously produced cAMP. Iontophoretic application of etazolate (25 nA) had highly consistent suppressing effects on spatial mnemonic activity in 10 of 12 PFC neurons. One example is shown in Figure 3B, in which etazolate dramatically inhibited spatial delay-related firing ($p < 0.0001$). The population response is shown in Figure 3F.

In contrast to Sp-cAMPS and etazolate, iontophoresis of the cAMP inhibitor, Rp-cAMPS (40–50 nA) specifically increased delay-related firing for the preferred direction in 8 of 12 neurons ($p < 0.001$, Figure 3C, population response in Figure 3E). This enhancing effect was reversed by subsequent coiontophoresis of Sp-cAMP ($p < 0.001$), consistent with actions via cAMP signaling. Thus, inhibition of cAMP actions had an effect similar to that of iontophoresis of guanfacine.

Guanfacine Enhances WM via Inhibition of cAMP

The enhancing effects of guanfacine on WM in rats has been reversed by coinfusion of Sp-cAMPS (Ramos et al., 2006). We examined whether the enhancing effects

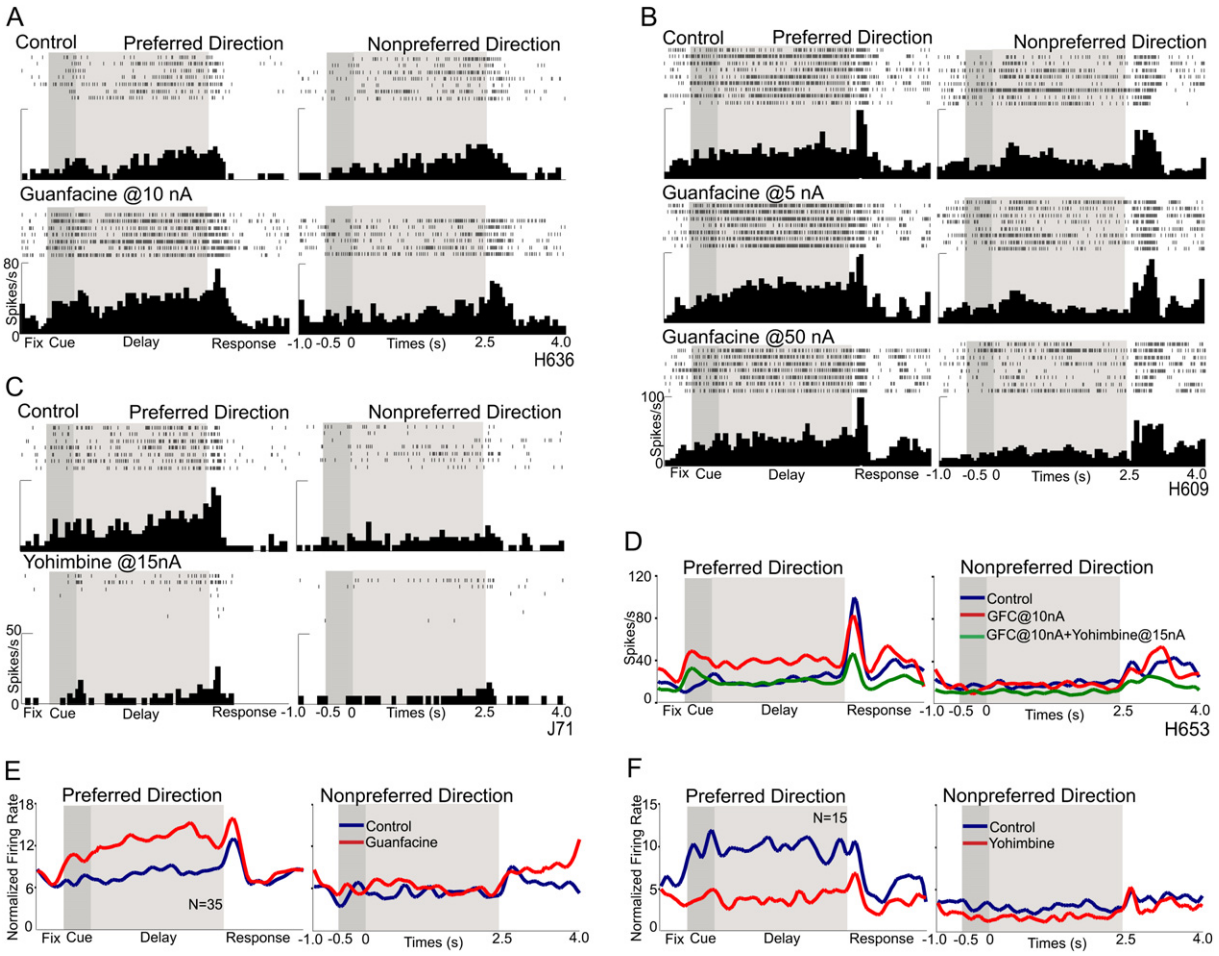

Figure 2. α2A-AR Stimulation Strengthens WM-Related Firing of PFC Neurons

(A) Iontophoretic application of the α2A-AR agonist, guanfacine, enhanced delay-related firing for a neuron with weak tuning under control conditions.

(B) Iontophoresis of a low dose of guanfacine increased delay-related firing in a well-tuned neuron as well, while a high dose was without effect.

(C) Iontophoresis of the α2-AR antagonist, yohimbine, decreased delay-related firing and eroded spatial tuning of a PFC neuron.

(D) Coiontophoresis of yohimbine with guanfacine reversed the enhancing effects of guanfacine on delay-related firing.

(E) Enhancing effect of guanfacine (red) on delay-related activity at the population level (35 neurons).

(F) Suppressive effect of yohimbine (red) on spatial delay-related activity at the population level (15 neurons).

of guanfacine on PFC neuronal firing are similarly reversed by Sp-cAMPS. As observed above, iontophoresis of guanfacine (10 nA) significantly increased delay-related firing for the preferred direction ($p < 0.001$, Figure 3D). Subsequent coiontophoresis of Sp-cAMPS (10 nA) with guanfacine (10 nA) significantly reversed the enhancing effects of guanfacine in six of nine cases ($p < 0.001$, Figure 3D). These results are consistent with guanfacine increasing delay-related firing through suppression of cAMP.

HCN Channels Are Key to Delay-Related Firing of PFC Neurons

As cAMP can increase the open state of HCN channels, we examined the role of Ih in WM by iontophoresing the HCN channel blocker, ZD7288. Low doses of ZD7288 (10 nA), like guanfacine or Rp-cAMPS, significantly increased delay-related firing for the preferred direction in 19 of 27 neurons. As with guanfacine, ZD7288 effects were most obvious in neurons with weak spatial tuning, however, small but consistent effects were also observed in well-tuned neurons with robust firing for the preferred direction under control conditions. For example, in Figure 4A, iontophoretic application of ZD7288 (5 nA) significantly increased delay-related firing for the preferred direction ($p < 0.001$), without altering baseline firing rates ($p > 0.05$), or firing for the nonpreferred direction ($p > 0.05$). ZD7288 had very robust enhancing effects on cells with weak mnemonic firing under control conditions. One example is shown in Figure 4B, in which application of ZD7288 induced dose-dependent effects, with a low dose (5 nA) significantly increasing delay-related firing

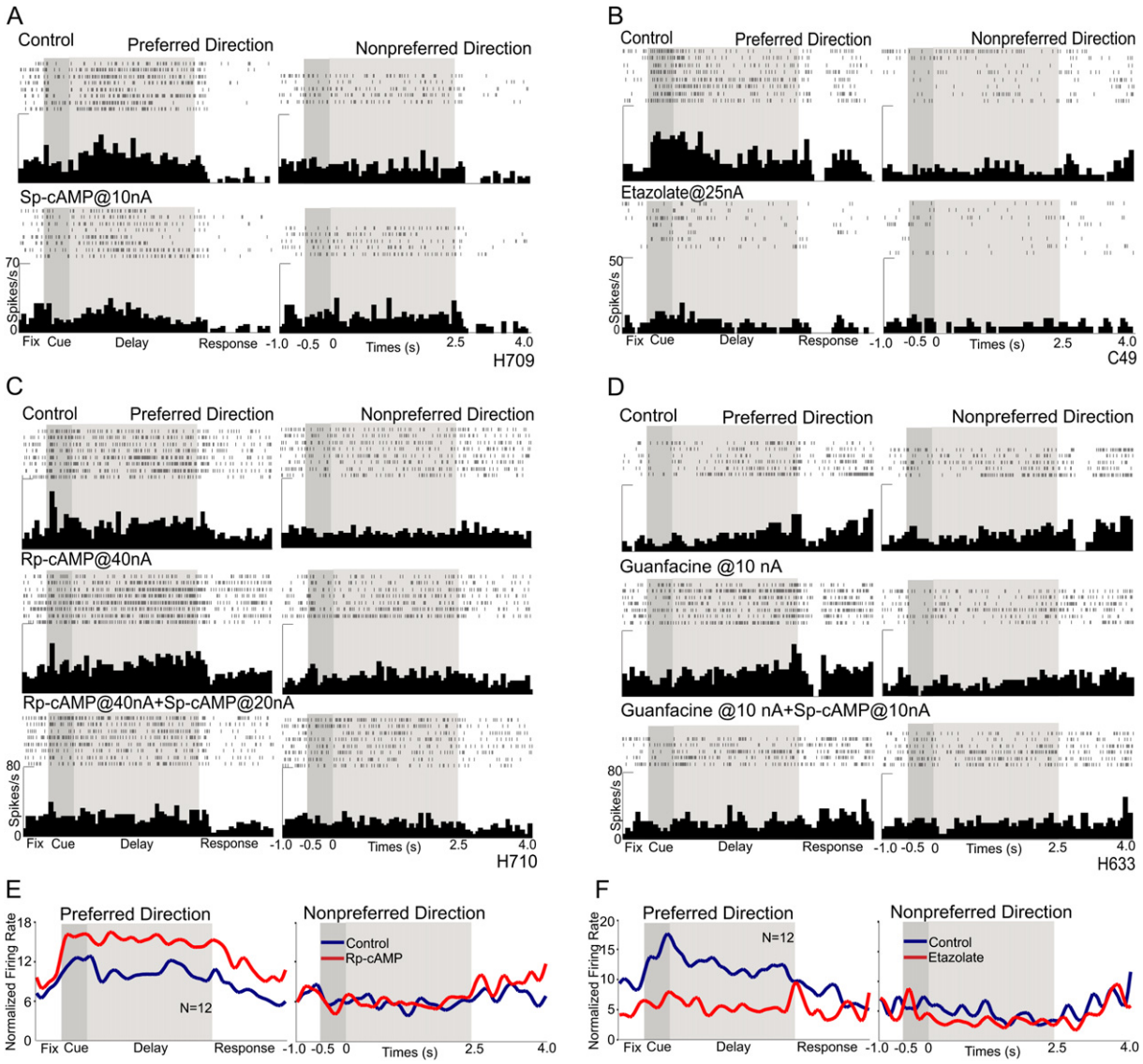

Figure 3. cAMP Suppresses the Delay-Related Firing of PFC Neurons

(A) Iontophoresis of the cAMP analog, Sp-cAMPS, decreased delay-related firing.

(B) Iontophoresis of the PDE4 inhibitor, etazolate, suppressed delay-related activity.

(C) Application of Rp-cAMPS enhanced delay-related activity, and coiontophoresis of Sp-cAMPS with Rp-cAMPS reversed the enhancing effects of Rp-cAMPS on delay-related firing.

(D) Coiontophoresis of Sp-cAMPS with guanfacine reversed the enhancing effects of guanfacine.

(E) Enhancing effect of Rp-cAMPS (red) on spatial delay-related activity at the population level (12 neurons).

(F) Suppressive effect of etazolate (red) on spatial delay-related activity at the population level (12 neurons).

for the preferred direction ($p < 0.001$). Subsequent application of ZD7288 at 10 nA further enhanced the delay-related activity for the preferred direction ($p < 0.0001$). This higher dose of ZD 7288 slightly increased the background firing rate, but produced greater delay-related firing for the preferred than the nonpreferred direction (ANOVA on percentage increase, $p < 0.01$). At the highest concentration (40 nA), ZD7288 decreased rather than increased firing (Figure 4B). These inhibitory effects likely arose from nonspecific blockade of glutamate receptors at high doses (Chen, 2004). The population response for low-dose ZD7288 application in 27 neurons is shown in Figure 4E.

A functional link between HCN channels and α2-ARs was examined by observing whether ZD7288 could reverse the effects of α2-AR blockade (Figure 4C). As observed above, iontophoretic application of yohimbine (15 nA) dramatically suppressed delay-related activity for the preferred direction ($p < 0.0001$). Subsequent

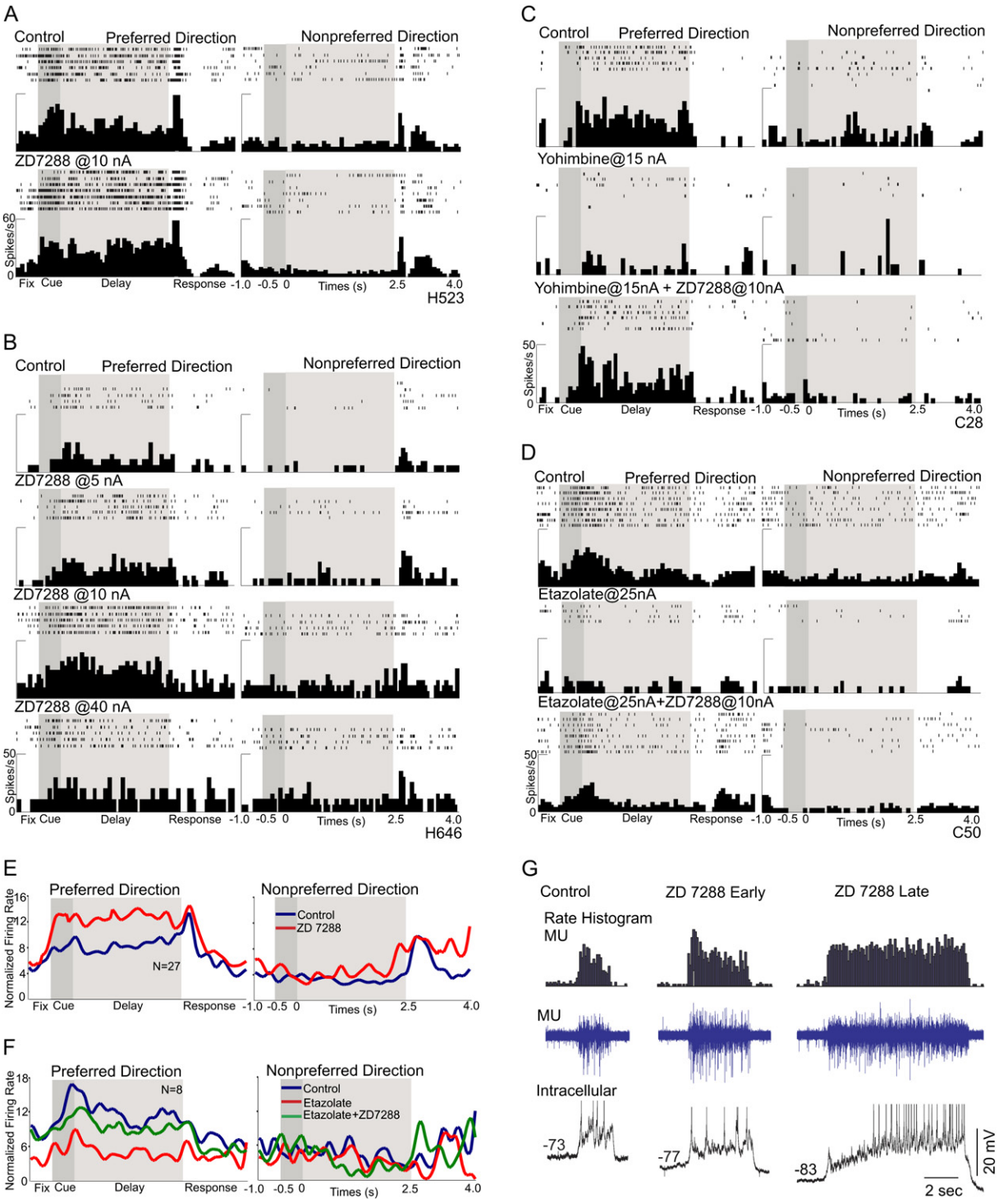

Figure 4. Blockade of HCN Channels Strengthens WM-Related Firing of PFC Neurons

(A) Iontophoresis of a low dose of ZD7288 increased delay-related firing in a well-tuned neuron.

(B) Iontophoretic application of ZD7288 caused a dose-dependent effect on delay-related firing in a neuron with weak tuning under control condition. ZD7288 at 5 nA and 10 nA enhanced delay-related activity, while a high dose (40 nA) eroded the spatial tuning.

(C) Coiontophoresis of ZD7288 with yohimbine reversed the suppressive effects of yohimbine on delay-related firing.

(D) Coiontophoresis of ZD7288 with etazolate reversed the suppressive effects of etazolate on delay-related firing.

(E) Enhancing effect of ZD7288 (red) on delay related activity at the population level (27 neurons).

coiontophoresis of ZD7288 significantly reversed the yohimbine response, restoring spatial mnemonic activity ($p < 0.001$). ZD7288 was able to reverse the suppressive effects of yohimbine in seven of nine cases ($p < 0.05$ for each case). These data support a functional interaction between α2-ARs and HCN channels at the physiological level.

We also examined functional interactions between HCN channels and cAMP. As shown in Figure 4D, the reduction in delay-related firing induced by the PDE4 inhibitor, etazolate ($p < 0.0001$) was fully reversed by coiontophoresis of ZD7288 ($p < 0.001$). ZD7288 reversed the suppressive effects of etazolate in six of eight cases ($p < 0.05$ for each case; Figure 4F). Thus, blockade of HCN channels restored delay-related firing under conditions of high endogenous cAMP levels induced by either PDE4 inhibition or α2-AR blockade. These electrophysiological results demonstrate the key role of α2A-cAMP-HCN signaling in permitting spatial mnemonic firing in PFC networks.

Reduction of HCN Activity in PFC Slices Enhances Recurrent Network Interactions

The cellular and network consequences of modulation of HCN channels was examined with intracellular and whole-cell recordings from layer V pyramidal cells simultaneously with extracellular multiple unit recordings in the ferret PFC in vitro (n = 55, see Figure 4G). Under normal conditions, these slices generate up and down states, consisting of repeating periods of recurrent network activity (Shu et al., 2003). Bath application of ZD7288 (20–50 μM; n = 10) resulted in a nearly 500% increase in duration of the recurrent network activity of the up state from an average of 0.84 (± 0.25) to 4.1 (± 1.3) s and an increase in up-state action potential discharge from 1.8 ± 1.7 Hz to 9.2 ± 4.9 Hz (n = 9). This ZD7288-induced enhancement of recurrent network activity occurred in conjunction with a progressive hyperpolarization of layer V pyramidal neurons (n = 12), an increase in apparent input resistance (from 18.6 ± 7.5 to 36 ± 10.8 mΩ, n = 10), and a marked enhancement of the amplitude of synaptic barrages of the up state from an average peak amplitude of 7.6 ± 2.7 mV to 20.7 ± 7.2 mV (n = 21 Figure 4G, lowest panel). These results reveal that reduction of the Ih results in significant enhancement of local recurrent network activity in cortical networks, presumably through enhanced effectiveness of dendritic synaptic potentials to initiate action potential activity (Fan et al., 2005; Magee, 1999; Nolan et al., 2004).

Reduced HCN Channel Activity in Rat PFC Improves Spatial WM Performance

The next study tested the hypothesis that reducing Ih in rat prelimbic PFC (Figure 5A) would improve performance of a spatial delayed alternation task sensitive to PFC lesions (Larsen and Divac, 1978). The prelimbic PFC displayed strong HCN1 immunoreactivity, with robust labeling of the apical dendrites in superficial layers (Figures 5B and 5C). Ih was then reduced through either (1) blockade of HCN channels with intra-PFC ZD7288 infusions or (2) knockdown of HCN1 channel expression in PFC.

The first experiment tested whether infusion of ZD7288 into prelimbic PFC would improve performance as previously seen with guanfacine (Ramos et al., 2006) and Rp-cAMPS (Ramos et al., 2003). Pilot experiments explored a wide range of ZD7288 doses (0.00001–0.1 μg/0.5 μl). Improvement was only observed in the low dose range; thus, the 0.0001 μg dose became the focus of the present study. ZD7288 was challenged with a low dose of the cAMP analog, Sp-cAMPS (0.21 nmol/0.5 μl), chosen to have no effect on its own. Results are shown in Figure 5D. Intra-PFC infusion of ZD7288 significantly improved performance, and this effect was blocked by co-infusion of Sp-cAMPS. 2-ANOVA-R analysis showed a significant main effect of ZD7288, ($F(1,4) = 23.64$, $p = 0.008$); a significant main effect of Sp-cAMPS, ($F(1,4) = 7.37$, $p = 0.05$); and a significant interaction between ZD7288 and Sp-cAMPS ($F(1,4) = 30.12$, $p = 0.005$). Planned comparisons showed that infusion of ZD7288 alone significantly improved accuracy compared to saline ($F(1,4) = 42.67$, $p = 0.003$). Sp-cAMPS infusion had no effect on its own ($F(1,4) = 1.24$, $p = 0.33$), but significantly reversed the enhancing effects of ZD7288 ($F(1,4) = 18.46$, $p = 0.01$; ZD7288 + Sp-cAMPS not different than saline: $F(1,4) = 0.02$, $p = 0.88$). Thus, HCN channel blockade enhanced WM at the behavioral and single-cell levels.

In the second experiment, HCN1 expression was knocked down by RNA interference in prelimbic PFC through infusion of one of two short hairpin-expressing viral constructs, shRNA-HCN1.1 or shRNA-HCN1.2 (Figure 5G; both were effective, and so behavioral results were combined). Performance was compared to rats infused with a scrambled, inactive viral construct (shRNA-scrHCN1). Rats infused with the active constructs showed no change for the first week following infusion (mean % correct ± SEM for scrambled: 72.3.4 ± 3.6; for HCN1: 70.2 ± 5.5%; $p > 0.7$), but then showed significant improvements in WM performance 11–19 days after viral infusion. A 2-ANOVA-R analysis showed a significant between subjects effect of viral construct (active versus scrambled: $F[1,6] = 9.57$, $p = 0.02$), a significant within subjects effect of time (pre- versus postinfusion performance: $F[1,6] = 24.61$, $p = 0.003$), and a significant interaction between viral construct and time after infusion ($F[1,6] = 23.5$, $p = 0.003$). As shown in Figure 5E, there was no difference between viral groups at baseline

(F) Coiontophoresis of ZD7288 with etazolate (green) reversed the suppressing effects of etazolate (red) on delay-related activity at the population level (8 neurons).

(G) Bath application of ZD-7288 resulted in a prolongation of the persistent activity of the up state in ferret PFC cortical slice in vitro as recorded simultaneously with extracellular multiple unit (MU; upper traces) and intracellular recording from layer 5 neurons (lower trace). This effect of ZD7288 was associated with a hyperpolarization of pyramidal neurons and a strengthening of the synaptic barrages mediating the recurrent network activity.

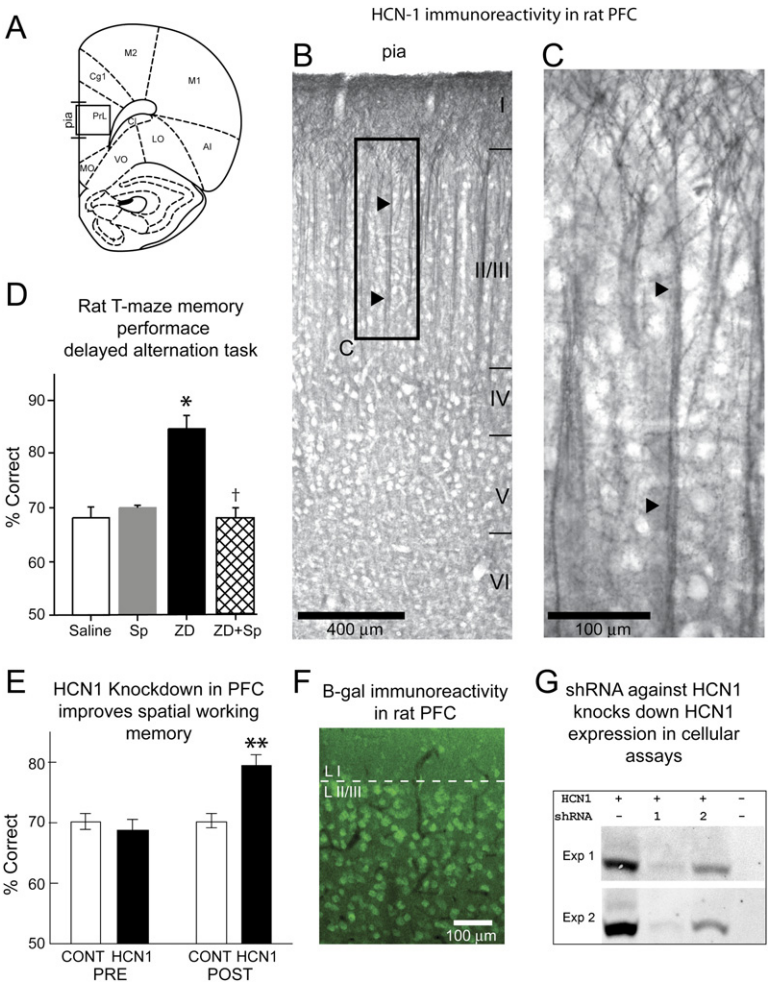

Figure 5. Blockade or Knockdown of HCN Channels in Rat PFC Improves WM

(A) Rat prelimbic PFC in coronal plane, modified from (Paxinos and Watson, 1997).

(B and C) Low- (B) and high-power (C) light microscopic demonstration of HCN-1 immunoreactivity in PFC. Arrowheads indicate densely labeled apical dendrites in layers II/III. Note that immunoreactivity increases in upper layer processes. The scale bar represents 0.4 mm (B); 0.1 mm (C).

(D) Blockade of HCN channels in PFC with infusions of ZD7288 (0.0001 μg/0.5 μl) improved WM performance. The improvement was blocked by coinfusion of the cAMP analog, Sp-cAMPS (0.21 nmol). Results represent mean ± SEM percent correct on the delayed alternation task; n = 5; *p = 0.003 compared to vehicle; †p = 0.01 compared to ZD7288.

(E) Knockdown of HCN1 channels in PFC significantly improved WM performance 11–19 days posttransduction compared to scrambled control; n = 8; **p = 0.0011 compared to scrambled construct.

(F) Representative example of viral expression in the PFC as indicated by β-galactosidase immunohistochemistry, visualized with Alexa Flour 488.

(G) Western blots confirmed shRNA against HCN1 knocks down HCN1 expression in cellular assays.

(F[1,6] = 1.03, p = 0.35), but a significant improvement in the active HCN1 viral group 11–19 days postinfusion (F[1,6] = 34.38, p = 0.0011). This is consistent with the time course of gene expression from AAV2 that we and others have observed, e.g., (Hommel et al., 2003). Postmortem analyses confirmed viral transduction of the prelimbic PFC (Figure 5F) and lack of expression of HCN1 in the rats receiving active construct (Figure S1).

HCN Channels and α2A-ARs Colocalize on Dendritic Spines

Ultrastructurally, HCN1 and the pore region of HCN (corresponding to HCN1 and/or HCN2 subunits in the cortex; (Notomi and Shigemoto, 2004) were predominantly detected in dendritic spines and the shafts of pyramidal dendrites (Figures 6A, 6B, and S2A–S2C). Immunoparticles in dendrites were clearly extrasynaptic (i.e., not localized at the active zone or within a 50 nm perisynaptic annulus). In favorable section planes, as in Figure 6B, HCN channels were observed at the base of emerging spines or, typically, the neck portion. This rather unusual localization could be followed in serial sections and is unlikely to occur as a diffusion artifact, as spine heads in continuity with HCN-immunoreactive necks were often themselves immunonegative. Note that in spine heads (Supplemental Figures 3A and 3B), HCN channels appeared both at extrasynaptic membranes and perisynaptically at the edge of asymmetric, presumably excitatory synapses.

α2A-AR-immunoreactive profiles in the neuropil included the spine-laden pyramidal dendrites, besides axonal and glial localization (Supplemental Figures 2D–2F; Aoki et al., 1998). Distal dendrites showed plasmalemmal but also cytoplasmic labeling, indicative of a rapid turnover from the plasma membrane. Similar to HCN, α2A-AR-immunoparticles in spines marked extrasynaptic and perisynaptic membranes flanking asymmetric synapses (Figure S3, compare S3D with S3B). In addition, we observed α2A-AR labeling intracellularly (Figure S3C) and rarely within the postsynaptic specialization per se. It is worth noting that both the head and the neck portion of spines were immunoreactive for α2A-ARs, as with HCN channels (Figure 6, compare 6C with 6B).

Dual immunolabeling confirmed the coexpression of HCN1 channels and α2A-ARs in spines and dendritic shafts at sites where emerging spines would come into focus. HCN1/α2A-AR labeling involved both the spine head

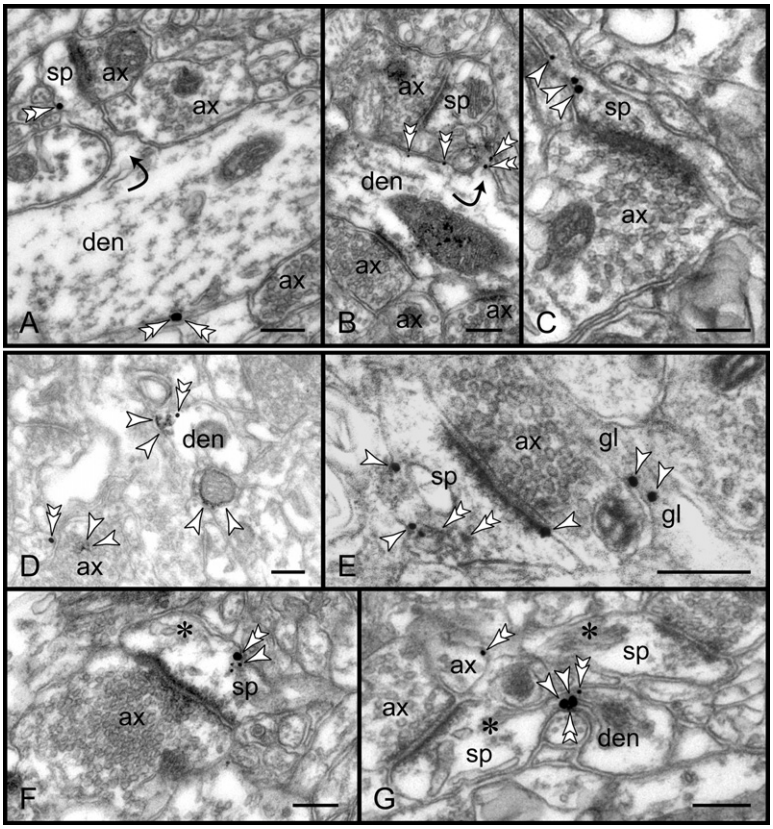

Figure 6. HCN Channels and α2A-ARs Are Colocalized in Dendritic Spines of Primate PFC

HCN channels (double arrowheads) and α2A-ARs (arrowheads) are colocalized in dendritic spines of primate PFC. HCN (A and B) and α2A-AR (C) immunoparticles mark extrasynaptic membranes in the spine head and neck region (compare [B] to [C]); curved arrows point to emerging spines. In dual labeling, α2A-AR was visualized with immunoperoxidase and HCN1 with silver-enhanced nanogold (D) or with reversal of the immunocytochemical sequence (E). Sequential gold enhancement of nanogold is shown in (F); (G) depicts the reverse procedure as in (E). HCN channels and α2A-ARs are coexpressed at extrasynaptic sites (E and F), including the spine neck (G), or where a dendrite tapers outwards, possibly to give rise to a spine (D). Singly labeled profiles in (D) attest to the specificity of dual immunolabeling; lead counterstaining was omitted to facilitate detection. Asterisks mark spine apparata. ax, axon; den, dendrite; gl, glial process; sp, spine. Scale bars represent 200 nm.

and the neck portion. This pattern was reproduced with reversal of the immunocytochemical sequence, and with both peroxidase/gold (Figures 6D and 6E) and dual gold (Figures 6F and 6G) immunotechniques. Thus, in superficial layers of monkey PFC, HCN1 channels and α2A-ARs are spatially coexpressed on spine membranes.

DISCUSSION

The current data provide evidence that HCN channels have powerful effects on PFC network firing properties and cognitive performance in animals performing WM tasks. Blockade of HCN channels with ZD7288 promoted persistent network activity and enhanced the spatial mnemonic firing of PFC neurons. Similar enhancing effects were observed with stimulation of α2A-ARs or inhibition of cAMP. Conversely, increasing cAMP signaling– either directly with Sp-cAMPS, or indirectly via blockade of α2-ARs or PDE4 inhibition– dramatically suppressed delay-related firing. Blockade of HCN channels restored mnemonic activity in cells with excessive cAMP signaling induced by either blockade of α2-ARs or PDE4 inhibition, thus demonstrating a functional interaction between α2-ARs, endogenous cAMP, and HCN modulation of PFC neuronal firing. Similar effects were observed at the behavioral level, where HCN channel blockade or HCN1 channel knockdown in PFC improved spatial WM performance. Ultrastructural localization of HCN channels and α2A-ARs indicates that they are ideally situated to modulate synaptic inputs onto PFC pyramidal neurons.

HCN Channels Are Positioned to Gate Cortico-Cortical Inputs in PFC Networks

HCN channels on spine extrasynaptic and perisynaptic membranes are ideally positioned for gating glutamatergic transmission mediated by axospinous synapses, including cortico–cortical inputs of the superficial PFC. When opened in the presence of cAMP, HCN channels would lower membrane resistance and shunt inputs to the spine. Due to the small cytosolic volume, HCN channels in the spine head –and especially those in the spine neck– are capable of "sensing" minute neurochemical changes in the milieu caused by the downstream effects of "colocalized" neurotransmitter receptors. Our ultrastructural data suggest that one such candidate receptor in PFC is the α2A-AR. It is noteworthy that the latter was found not only in the head but also in the neck of spines on both perisynaptic and extrasynaptic membranes, and dual labeling confirmed the spatial coexpression of HCN1 and α2A-ARs. α2A-ARs inhibit cAMP production via Gi signaling and thus could have a powerful influence on the open state of nearby HCN channels. Inadequate stimulation of α2A-ARs would result in elevated cytosolic cAMP levels, opening Ih channels, and selectively disconnecting

axospinous inputs to cortical pyramids. Therefore, cytosol compartmentalization in the spine, and the coexpression of HCN channels with α2A-ARs on spine membranes, may provide a cellular basis for altering the strength of excitatory transmission at individual axospinous synapses, thus modulating circuit connectivity in PFC.

α2A-AR Inhibition of cAMP-HCN Signaling Enhances Spatially Tuned, Delay-Related Firing of PFC Neurons

The functional implications suggested by immunoelectron microscopy were supported by our physiological data. Delay-related firing arises from reverberating, excitatory circuits in PFC, and depends on the functional connectivity of neurons with shared spatial tuning. The current study found that agents, which (1) stimulate α2A-ARs, (2) inhibit cAMP signalling, or (3) block HCN channels, all increase delay-related firing for the preferred direction, consistent with increased functional connectivity under conditions where HCN channels are closed. Conversely, delay-related firing collapsed in the presence of agents that blocked α2A-ARs or increased cAMP signaling, consistent with reduced functional connectivity when cAMP opens HCN channels. These modulatory effects were very powerful: extremely low doses selectively altered delay-related firing for the preferred direction, while slightly higher doses had more generalized effects on firing, consistent with perturbations in network firing. Parallel results were observed in vitro, and at the behavioral level, where PFC infusions of guanfacine (Ramos et al., 2006) or ZD7288, or knockdown of HCN1 expression in PFC, all improved WM performance, while agents that blocked α2A-ARs (Li and Mei, 1994) or accentuated cAMP signaling (Taylor et al., 1999) impaired WM. It is remarkable to have such confluence between behavioral and electrophysiological findings.

ZD7288 is currently the most selective HCN antagonist available, and, as such, has become the standard pharmacological method for assessing Ih mechanisms, e.g., (Fan et al., 2005). However, it has recently been noted that at higher doses ZD7288 becomes nonselective, producing AMPA and NMDA glutamate receptor blockade (Chen, 2004). The inhibition of cell activity at higher ZD7288 concentrations (25–40 nA) in the current study could be consistent with reduced glutamate receptor excitation. A similar profile was observed in our behavioral data, where pilot studies showed that higher doses of ZD7288 were ineffective, whereas a very low dose consistently improved WM performance.

Physiological interactions between α2A-ARs and HCN channels were observed, consistent with their coexpression in spines: The collapse in memory fields induced by the α2A-AR antagonist, yohimbine, was reversed by the HCN channel blocker, ZD7288. HCN channel blockade similarly reversed the suppressive effects of the PDE4 inhibitor, etazolate. Thus, iontophoresis of yohimbine, Sp-cAMPS or etazolate, all induced an immediate collapse in memory fields, likely due to a reduction in recurrent excitatory drive in the PFC network. The blockade of HCN channels with ZD7288 restored a normal firing pattern. It should be noted that these agents are not likely competing at the same individual channel; rather, it is likely that ZD7288 and Sp-cAMPS (or cAMP per se) each alter the open state of a subset of HCN channels, and we record the integration of this population response. It is striking that very low doses can have such rapid and robust effects on cell firing, revealing a powerful mechanism for the dynamic regulation of PFC microcircuits.

HCN Channels Have Distinct Actions in PFC versus Hippocampus versus Cerebellum

Recent studies of HCN1 knockout mice have revealed distinct roles of Ih in cerebellum and hippocampus, and it is instructive to compare the current results with these important findings. In cerebellar Purkinje cells, HCN1 channels mediate an inward current that stabilizes the integrative properties of the cell and ensures that their input-output function is independent of previous activity (Nolan et al., 2003). HCN1 currents allow Purkinje cells to integrate information very quickly, consistent with the rapid time scale of cerebellar mechanisms (ibid). However, the influence of HCN channels in cerebellum occurs only when Purkinje cells are hyperpolarized. In contrast, pyramidal cells in hippocampus and PFC have a lower resting membrane potential, and thus HCN channels may play a role under resting conditions in these cells (Nolan et al., 2004). Pyramidal cells in PFC and hippocampus share other properties: HCN1 channels are localized on their distal dendrites, and, when opened, appear to shunt synaptic inputs onto those distal locations (Magee, 1999; Nolan et al., 2004). However, there are important differences between CA1 and PFC neurons as well. In hippocampus, high levels of cAMP are essential for long-term potentiation and memory consolidation, leading to long-lasting changes in synaptic architecture (cAMP also plays a beneficial role when hippocampus interacts with PFC under conditions when delay lengths are very long, see (Runyan and Dash, 2005). In contrast, the WM operations of the PFC depend on the transient activation of microcircuits that are disrupted by high levels of cAMP. Thus, cAMP-HCN signaling may play an especially important role in PFC.

Model of α2A-cAMP-HCN Modulation of PFC Networks

Figure 7 illustrates a model whereby HCN channels on spines of PFC distal pyramidal dendrites modulate the efficacy of excitatory inputs. Pyramidal cells form reverberating circuits through mutual, axospinous excitatory connections. HCN channels are localized on the spine neck or near excitatory synapses on spine head membranes. When HCN channels are open in the presence of cAMP, they pass Ih that lowers membrane resistance and effectively shunts synaptic input, reducing the functional connectivity of the network (Figure 7A). NE regulates this process. We have shown α2A-ARs and HCN1 channels

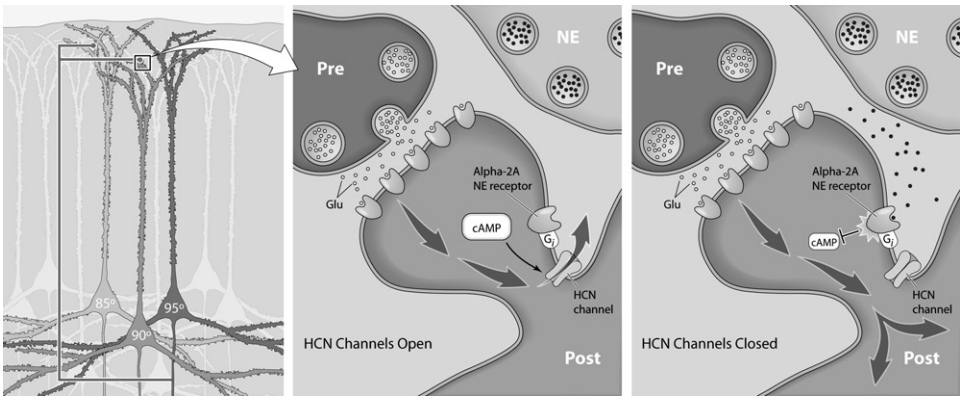

Figure 7. A Model of α2A-cAMP-HCN Regulation of PFC Microcircuits

HCN channel opening shunts synaptic inputs onto dendritic spines and reduces network activity. α2A-AR stimulation inhibits the production of cAMP and increases the efficacy of cortical inputs.

on the same spine membranes. Stimulation of α2A-ARs, e.g., with guanfacine, inhibits the production of cAMP, closing HCN channels and increasing the efficacy of synaptic inputs, thus strengthening the functional connectivity of PFC microcircuits (Figure 7B). Thus, α2A-cAMP-HCN signaling provides a mechanism for dynamically regulating the strength of PFC networks.

The present research further suggests that Gs-coupled receptors may temporarily suppress neurotransmission by activating cAMP production, opening HCN channels and shunting synaptic inputs. For example, dopamine D1 receptors (D1Rs) are coupled to Gs, and are also concentrated on spines in superficial PFC (Smiley et al., 1994). We have recently observed that moderate levels of D1R stimulation suppress firing for nonpreferred spatial directions via a cAMP-mediated mechanism (Vijayraghavan et al., 2007). It is not known if this suppression involves opening of HCN channels. If so, it is possible that α2A-ARs amplify inputs for preferred directions by selectively closing HCN channels on spines receiving inputs from neurons with shared spatial preferences, while D1Rs may shunt inputs from neurons tuned to nonpreferred directions. Thus, the open state of HCN channels may determine which pattern of microcircuits are functionally connected at any one time to appropriately regulate behavior and thought based on immediate cognitive demands.

α2A-AR-cAMP-HCN Signaling Is a Function of Arousal State

α2A-cAMP-HCN signaling in superficial cortical layers likely regulates the strength of PFC function based on the animal's state of arousal. Low levels of NE cell firing during drowsy conditions (Aston-Jones et al., 1999) may lead to insufficient NE stimulation of α2A-ARs, inadequate inhibition of cAMP, and impaired WM. Conversely, exposure to uncontrollable stress impairs WM via excessive catecholamine release (Arnsten, 2000). Similar effects are observed at the cellular level, where memory fields collapse under neurochemical conditions induced by stress: e.g., etazolate, Sp-cAMPS, (Figure 3) or high levels of D1R stimulation activating cAMP (Vijayraghavan et al., 2007). Thus, under conditions of uncontrollable stress, cortico-cortical connections of superficial PFC would be functionally disconnected, rendering the PFC "decorticate". This process may be exacerbated in patients with alterations in genes that regulate cAMP signaling, e.g., COMT (Egan et al., 2001) or DISC1 (Millar et al., 2005), increasing vulnerability to PFC dysfunction in illnesses such as schizophrenia that are worsened by stress exposure. Intriguingly, DISC1 protein has been localized to dendritic spines in human PFC, (Kirkpatrick et al., 2006), suggesting that it may normally regulate Ih, but may inadequately suppress cAMP levels in spines of patients with schizophrenia. Guanfacine has recently been shown to strengthen PFC cognitive function in patients with schizotypal disorder (McClure et al., 2006), as well as those with ADHD (Scahill et al., 2001; Taylor and Russo, 2001). The present data suggest that some of these enhancing effects may result from reduced cAMP production and the closure of HCN channels. Thus, we are able to reveal the mechanism of action of a psychotropic medication at the level of an ion channel, and observe the powerful influence of arousal pathways on cortical microcircuitry.

EXPERIMENTAL PROCEDURES

All procedures were approved by the Yale IACUC. Additional details are provided in the Supplemental Data.

Single Neuron Recording and Iontophoresis in Monkeys Performing a Spatial WM Task

Studies were performed on four adult male rhesus monkeys trained on the spatial ODR task. Neurons were recorded from area 46 of the dorsolateral PFC (Figure 1). Iontophoretic electrodes comprised of a 20 μm carbon fiber (ELSI, San Diego, CA) inserted in a seven-barrel nonfilamented capillary glass (Friedrich and Dimmock, Millville, NJ). Signals were acquired using Spike2 (CED, Cambridge, UK). Drugs

were delivered using a Neurophore BH2 system (Medical Systems, Greenvale, NY). Details are provided in Vijayraghavan et al. (2007) and in the Supplemental Data.

Guanfacine, yohimbine, ZD7288 (Tocris, Ellisville, MO), and etazolate (Sigma, St. Louis, MO) were dissolved in water (0.01 M, [pH 3.5]). Sp-cAMPS and Rp-cAMPS (Sigma) were dissolved in water (0.01 M, [pH 9]). We examined spatially tuned task-related activity using two-way ANOVA for: (1) different task epochs (cue, delay, response versus fixation) and (2) different cue locations. We assessed the effects of drug application using one-way ANOVAS.

In Vitro Recordings from PFC Slices

Methods for extracellular multiple unit and intracellular recording in ferret PFC slices have been detailed elsewhere (Shu et al., 2003). Slices (0.4 mm) from 2- to 4-month-old ferret PFC were maintained in either an interface or submerged chamber (35°C–36°C) in a slice solution containing (in mM): NaCl, 126; KCl, 3.1; $MgSO_4$, 1; $NaHPO_4$, 1.25; $CaCl_2$, 1; $NaHCO_3$, 26; dextrose, 10, and aerated with 95% O_2, 5% CO_2 to a final pH of 7.4. Simultaneous extracellular multiple unit and intracellular recordings were performed in layer V with the electrodes approximately 100 μm of one another. Intracellular micropipettes contained 2 M potassium acetate, while whole-cell recording pipettes contained (in mM) KGluconate 140, KCl 3, $MgCl_2$ 2, Na_2ATP 2, HEPES 10, and EGTA 0.2.

Assessment of Spatial WM Performance in Rats

Male Sprague Dawley rats (240–260 g; Taconic, Germantown, NY) were trained on the delayed alternation task as described in Ramos et al. (2003). Guide cannulae were implanted dorsal in prelimbic PFC (AP: +3.2 mm; ML: ±0.75 mm; DV: −4.2 mm). For infusions, needles reached to 4.5 mm DV; infused at 0.25 μL/min for 2 min. Drug or vehicle was administered in a counterbalanced order with at least 1 week between infusions. ZD7288 was dissolved in saline to a dose of 0.0001 μg/0.5 μl. Sp-cAMPS was dissolved in sterile phosphate-buffered saline (PBS) at 0.21 nmol, a dose with no effect on its own, but sufficient to reverse the effects of guanfacine (Ramos et al., 2006). The experimenter was blind to treatment.

Viral Knockdown of HCN1

The coding region of HCN1 was amplified from rat brain cDNA, cloned into pSTBlue-1 (Novagen, San Diego CA), sequenced, and subcloned into pAAV-MCS (Stratagene, La Jolla, CA) to create pAAV-HCN1. A vector containing an H1 promoter for shRNA expression and a CMV promoter for lacZ expression flanked by AAV ITR sequences (pAAV-lacZ-shRNA) was created to allow viral expression of shRNAs. Two sets of shRNAs constructs (shRNA-HCN1.1 and shRNA-HCN1.2) directed against HCN1 were generated and tested in HEK293 cells by cotransfection with pAAV-HCN1. A control shRNA viral construct containing a scrambled sequence (shRNA-scrHCN1) was created with an identical nucleotide composition as the shRNA-HCN1.1 target sequence with no homology to any mammalian gene in the Genbank database. AAV2 virus was produced by transfection of HEK293 cells with pAAV-HCN1 or one of the pAAV-lacZshRNA constructs, and pDG (kindly provided by Drs. M. Kay and D. Grimm, Stanford University) essentially as described by (Auricchio et al., 2001). Viral titers were determined by determining viral genome copy number and by infectious titer assays in HEK293 cells.

Rats were implanted with cannula, and trained until achieving baseline performance of ~70% correct for at least 5 consecutive days. The active or scrambled virus (5 μl) was infused into the prelimbic PFC at a rate of 0.25 μl/min. WM was assessed the following day and for the subsequent 3 weeks. Rats were perfused and viral transduction was confirmed in PFC with a monoclonal antibody against β-galactosidase (Mouse anti β-gal 1:400, overnight, RT; Promega Corp., Madison, WI) followed by a secondary antibody (Goat anti-mouse conjugated to Alexa Flour 488, 1:400, 4 hr, RT; Invitrogen/Molecular Probes, Carlsbad, CA). Antibodies were prepared in 0.1 M PB containing 0.1% Triton X and 2% normal goat serum. All behavioral studies were performed blind to treatment.

HCN and α2A-AR Localization in Monkey PFC–Electron Microscopic Studies

Monkey PFC tissue (n = 3) was processed as described in the Supplemental Data and in (Paspalas and Goldman-Rakic, 2004). For single HCN1, HCN-pore or α2A-AR immunocytochemistry, primary antibodies were complexed with nanogold conjugates, either directly or using biotinylated bridging antibodies. For dual immunolabeling, we used combinations of enzymatic and/or gold-based immunotechniques, and reversal of the immunocytochemical sequence (Figures 6D–6G); see Paspalas and Goldman-Rakic (2004), and Table S3 for a list of all immunoprobes. Sections were processed for electron microscopy and layers I–III of area 46 were sampled for analysis under a JEM 1010 (Jeol, Tokyo, Japan) transmission electron microscope at 80 KV. Immunoreactive structures were digitally captured with a Bio-Scan 792 (Gatan, Pleasanton, CA). Methods for light microscopic localization in rats are described in the Supplemental Data.

Supplemental Data

Supplemental Data include Supplemental Experimental Procedures, Supplemental References, three tables, and three figures and can be found with this article online at http://www.cell.com/cgi/content/full/129/2/397/DC1/.

ACKNOWLEDGMENTS

This research was supported by R37 AG06036, a research grant from Shire Pharmaceuticals, and an award from the Kavli Institute of Neuroscience at Yale University to A.F.T.A.; by R37 NS026143 to D.A.M.; by P50MH068789 to A.F.T.A. and D.A.M.; and in part by a NARSAD Young Investigator Award and by Grant K12RR17594 from the NCRR to A.S. Dr. Arnsten and Yale University have a license agreement with Shire Pharmaceuticals for the development of guanfacine for the treatment of Attention Deficit Hyperactivity Disorder. Yale University has submitted a patent application on the use of HCN blockers for the treatment of PFC cognitive deficits based on the above data. We are grateful to Lisa Ciavarella, Tracy Sadlon, Sam Johnson, and Jessica Thomas for their invaluable technical support. The authors are indebted to Dr. R. Shigemoto for generously providing the guinea pig HCN1 antibody.

Received: November 14, 2006
Revised: January 9, 2007
Accepted: March 2, 2007
Published: April 19, 2007

REFERENCES

Aoki, C., Venkatesan, C., Go, C.-G., Forman, R., and Kurose, H. (1998). Cellular and subcellular sites for noradrenergic action in the monkey dorsolateral prefrontal cortex as revealed by the immunocytochemical localization of noradrenergic receptors and axons. Cereb. Cortex *8*, 269–277.

Arnsten, A.F.T. (2000). Stress impairs PFC function in rats and monkeys: Role of dopamine D1 and norepinephrine alpha-1 receptor mechanisms. Prog. Brain Res. *126*, 183–192.

Arnsten, A.F.T., Cai, J.X., and Goldman-Rakic, P.S. (1988). The alpha-2 adrenergic agonist guanfacine improves memory in aged monkeys without sedative or hypotensive side effects. J. Neurosci. *8*, 4287–4298.

Arnsten, A.F.T., and Goldman-Rakic, P.S. (1985). Alpha-2 adrenergic mechanisms in prefrontal cortex associated with cognitive decline in aged nonhuman primates. Science *230*, 1273–1276.

Aston-Jones, G., Rajkowski, J., and Cohen, J. (1999). Role of locus coeruleus in attention and behavioral flexibility. Biol. Psychiatry *46*, 1309–1320.

Auricchio, A., Hildinger, M., O'Connor, E., Gao, G.P., and Wilson, J.M. (2001). Isolation of highly infectious and pure adeno-associated virus type 2 vectors with a single-step gravity-flow column. Hum. Gene Ther. *12*, 71–76.

Chen, C. (2004). ZD7288 inhibits postsynaptic glutamate receptor-mediated responses at hippocampal perforant path-granule cell synapses. Eur. J. Neurosci. *19*, 643–649.

Chen, S., Wang, J., and Siegelbaum, S.A. (2001). Properties of hyperpolarization-activated pacemaker current defined by coassembly of HCN1 and HCN2 subunits and basal modulation by cyclic nucleotide. J. Gen. Physiol. *117*, 491–504.

Day, M., Carr, D.B., Ulrich, S., Ilijic, E., Tkatch, T., and Surmeir, D.J. (2005). Dendritic excitability of mouse frontal cortex pyramidal neurons is shaped by the interaction among HCN, Kir2, and Kleak channels. J. Neurosci. *25*, 8776–8787.

Egan, M.F., Goldberg, T.E., Kolachana, B.S., Callicott, J.H., Mazzanti, C.M., Straub, R.E., Goldman, D., and Weinberger, D.R. (2001). Effect of COMT Val108/158 Met genotype on frontal lobe function and risk for schizophrenia. Proc. Natl. Acad. Sci. USA *98*, 6917–6922.

Fan, Y., Fricker, D., Brager, D.H., Chen, X., Lu, H.C., Chitwood, R.A., and Johnston, D. (2005). Activity-dependent decrease of excitability in rat hippocampal neurons through increases in I(h). Nat. Neurosci. *8*, 1542–1551.

Franowicz, J.S., Kessler, L., Dailey-Borja, C.M., Kobilka, B.K., Limbird, L.E., and Arnsten, A.F.T. (2002). Mutation of the alpha2A-adrenoceptor impairs working memory performance and annuls cognitive enhancement by guanfacine. J. Neurosci. *22*, 8771–8777.

Fuster, J.M. (1985). The prefrontal cortex, mediator of cross-temporal contingencies. Hum. Neurobiol. *4*, 169–179.

Goldman-Rakic, P.S. (1995). Cellular basis of working memory. Neuron *14*, 477–485.

Goldman-Rakic, P.S., Lidow, M.S., and Gallager, D.W. (1990). Overlap of dopaminergic, adrenergic, and serotonergic receptors and complementarity of their subtypes in primate prefrontal cortex. J. Neurosci. *10*, 2125–2138.

Hommel, J.D., Sears, R.M., Georgescu, D., Simmons, D.L., and DiLeone, R.J. (2003). Local gene knockdown in the brain using viral-mediated RNA interference. Nat. Med. *9*, 1539–1544.

Jakala, P., Riekkinen, M., Sirvio, J., Koivisto, E., Kejonen, K., Vanhanen, M., and Riekkinen, P.J. (1999). Guanfacine, but not clonidine, improves planning and working memory performance in humans. Neuropsychopharmacology *20*, 460–470.

Kirkpatrick, B., Xu, L., Cascella, N., Ozeki, Y., Sawa, A., and Roberts, R.C. (2006). DISC1 immunoreactivity at the light and ultrastructural level in the human neocortex. J. Comp. Neurol. *497*, 436–450.

Kritzer, M.F., and Goldman-Rakic, P.S. (1995). Intrinsic circuit organization of the major layers and sublayers of the dorsolateral prefrontal cortex in the rhesus monkey. J. Comp. Neurol. *359*, 131–143.

Larsen, J.K., and Divac, I. (1978). Selective ablations within the prefrontal cortex of the rat and performance of delayed alternation. Physiolog. Psychol. *6*, 15–17.

Li, B.-M., Mao, Z.-M., Wang, M., and Mei, Z.-T. (1999). Alpha-2 adrenergic modulation of prefrontal cortical neuronal activity related to spatial working memory in monkeys. Neuropsychopharmacology *21*, 601–610.

Li, B.-M., and Mei, Z.-T. (1994). Delayed response deficit induced by local injection of the alpha-2 adrenergic antagonist yohimbine into the dorsolateral prefrontal cortex in young adult monkeys. Behav. Neural Biol. *62*, 134–139.

Lörincz, A., Notomi, T., Tamas, G., Shigemoto, R., and Nusser, Z. (2002). Polarized and compartment-dependent distribution of HCN1 in pyramidal cell dendrites. Nat. Neurosci. *5*, 1185–1193.

Magee, J.C. (1999). Dendritic Ih normalizes temporal summation in hippocampal CA1 neurons. Nat. Neurosci. *2*, 508–514.

Mao, Z.-M., Arnsten, A.F.T., and Li, B.-M. (1999). Local infusion of alpha-1 adrenergic agonist into the prefrontal cortex impairs spatial working memory performance in monkeys. Biol. Psychiatry *46*, 1259–1265.

McAllister, T.W., Flashman, L.A., Sparling, M.B., and Saykin, A.J. (2004). Working memory deficits after traumatic brain injury: catecholaminergic mechanisms and prospects for treatment–a review. Brain Inj. *18*, 331–350.

McClure, M.M., Barch, D.M., Romero, M.J., Harvey, P.D., and Siever, L.J. (2006). The effects of guanfacine on context processing abnormalities in schizotypal personality disorder. Biol. Psychiatry, in press.

Millar, J.K., Pickard, B.S., Mackie, S., James, R.S., Christie, S., Buchanan, S.R., Malloy, M.P., Chubb, J.E., Huston, E., Baillie, G.S., et al. (2005). DISC1 and PDE4B are interacting genetic factors in schizophrenia that regulate cAMP signaling. Science *310*, 1187–1191.

Miller, E.K., Erickson, C.A., and Desimone, R. (1996). Neural mechanisms of visual working memory in prefrontal cortex of the macaque. J. Neurosci. *16*, 5154–5167.

Nolan, M.F., Malleret, G., Dudman, J.T., Buhl, D.L., Santoro, B., Gibbs, E., Vronskaya, S., Buzsaki, G., Siegelbaum, S.A., Kandel, E.R., and Morozov, A. (2004). A behavioral role for dendritic integration: HCN1 channels constrain spatial memory and plasticity at inputs to distal dendrites of CA1 pyramidal neurons. Cell *119*, 719–732.

Nolan, M.F., Malleret, G., Lee, K.H., Gibbs, E., Dudman, J.T., Santoro, B., Yin, D., Thompson, R.F., Siegelbaum, S.A., Kandel, E.R., and Morozov, A. (2003). The hyperpolarization-activated HCN1 channel is important for motor learning and neuronal integration by cerebellar Purkinje cells. Cell *115*, 551–564.

Notomi, T., and Shigemoto, R. (2004). Immunohistochemical localization of Ih channel subunits, HCN1–4, in the rat brain. J. Comp. Neurol. *471*, 241–276.

Paspalas, C.D., and Goldman-Rakic, P.S. (2004). Microdomains for dopamine volume neurotransmission in primate prefrontal cortex. J. Neurosci. *24*, 5292–5300.

Paxinos, G., and Watson, C. (1997). The rat brain in stereotaxic coordinates, 3rd edn (New York: Academic Press).

Poolos, N.P., Migliore, M., and Johnston, D. (2002). Pharmacological upregulation of h-channels reduces the excitability of pyramidal neuron dendrites. Nat. Neurosci. *5*, 767–774.

Ramos, B., Birnbaum, S.B., Lindenmayer, I., Newton, S.S., Duman, R., and Arnsten, A.F.T. (2003). Dysregulation of protein kinase A signaling in the aged prefrontal cortex: New strategy for treating age-related cognitive decline. Neuron *40*, 835–845.

Ramos, B., Stark, D., Verduzco, L., van Dyck, C.H., and Arnsten, A.F.T. (2006). Alpha-2A-Adrenoceptor stimulation improves prefrontal cortical regulation of behavior through inhibition of cAMP signaling in aging animals. Learn. Mem. *13*, 770–776.

Runyan, J.D., and Dash, P.K. (2005). Distinct prefrontal molecular mechanisms for information storage lasting seconds versus minutes. Learn. Mem. *12*, 232–238.

Scahill, L., Chappell, P.B., Kim, Y.S., Schultz, R.T., Katsovich, L., Shepherd, E., Arnsten, A.F.T., Cohen, D.J., and Leckman, J.F. (2001). Guanfacine in the treatment of children with tic disorders and ADHD: A placebo-controlled study. Am. J. Psychiatry *158*, 1067–1074.

Shu, Y.-S., Hasenstaub, A., Badoual, M., Bal, T., and McCormick, D.A. (2003). Barrages of synaptic activity control the gain and sensitivity of cortical neurons. J. Neurosci. *23*, 10388–10401.

Smiley, J.F., Levey, A.I., Ciliax, B.J., and Goldman-Rakic, P.S. (1994). D1 dopamine receptor immunoreactivity in human and monkey cerebral cortex: predominant and extrasynaptic localization in dendritic spines. Proc. Natl. Acad. Sci. USA *91*, 5720–5724.

Taylor, F.B., and Russo, J. (2001). Comparing guanfacine and dextroamphetamine for the treatment of adult Attention Deficit-Hyperactivity Disorder. J. Clin. Psychopharmacol. *21*, 223–228.

Taylor, J.R., Birnbaum, S.G., Ubriani, R., and Arnsten, A.F.T. (1999). Activation of protein kinase A in prefrontal cortex impairs working memory performance. J. Neurosci. (Online) *19*, RC23.

Ulens, C., and Tytgat, J. (2001). Functional heteromerization of HCN1 and HCN2 pacemaker channels. J. Biol. Chem. *276*, 6069–6072.

Vijayraghavan, S., Wang, M., Birnbaum, S.G., Bruce, C.J., Williams, G.V., and Arnsten, A.F.T. (2007). Inverted-U dopamine D1 receptor actions on prefrontal neurons engaged in working memory. Nat. Neurosci. *10*, 376–384.